Astron. Astrophys. 319, 788–795 (1997)

ASTRONOMY
AND
ASTROPHYSICS

Hα detection of a clump of distant HII regions in the Milky Way⋆

D. Russeil[1]

Observatoire de Marseille, 2 Place Le Verrier, F-13248 Marseille Cedex 04, France

Received 9 February 1996 / Accepted 5 September 1996

Abstract. A group of 8 HII regions has been detected at a distance of 10 kpc from the Sun at galactic longitude 298°, using Hα wavelength observations. The observations were made with a scanning Fabry-Perot interferometer to provide a detailed Hα profile, which enables us to separate these distant HII regions from the 3 other layers of ionized gas seen along the line of sight. A comparison of 5 GHz continuum and IRAS data allows us to analyse the nature of each source. Most of the distant HII regions were already known as radio sources or IRAS sources but one of them has no radio or IRAS counterpart. Inversely, IRAS sources without radio continuum nor an Hα counterpart have been detected. Closer to us, on the same line of sight, we detected diffuse Hα emission linking the Sagittarius arm with the Carina arm at a distance of about 2.5 kpc, where no usual tracer of spiral structure had previously been found. The HII region RCW 64, also seen in this direction, seems to be located between the two main spiral arms.

Key words: interstellar medium: HII regions – Galaxy: structure – infrared: ISM: continuum – radio continuum

1. Introduction

In external spiral galaxies the star formation complexes can be detected optically far from the galactic center. However in our Galaxy, optical star formation tracers situated at large distances from the Sun are not easily observable because of interstellar extinction. As a result, a large part of the Galaxy is optically hidden, principally toward the galactic center. Fortunately, in some particular directions, distant HII regions can be detected. This is the case toward galactic longitude l = 298°, where the line of sight is found between two spirals arms, implying weak absorption effects. Eight distant HII regions in the Carina arm have been detected at this longitude using a 36 cm telescope in La Silla devoted to an Hα Survey of the Milky Way. Never before have so many HII regions been optically observed at such a distance (10 kpc) in the same field. Well known in the radio continuum (Haynes et al. 1978), only two of these had already been optically detected: 298.2 - 0.3 (Georgelin et al. 1979) and 298.19 - 0.77 (Henize 1967).

Some HII regions have been detected in Hα at large distances. For example W 58G at a distance of 12.4 kpc (Georgelin et al. 1988) and the farthest one detected by Degeus et al. (1993) at a distance of 21 kpc. These very distant regions allow us to probe the galactic gravitational potential but such HII regions are rare and isolated. The HII regions detected near l = 298° are spatially grouped which suggests a common origin and behaviour.

The comparison of Hα maps with maps at other wavelengths allow a detailed analysis of each source. In particular, the infrared observations help to form an understanding of the Hα detections and reveal interesting object which have no Hα nor a radio emission counterpart.

After the description of the observations and results presented in Sect. 2, Sect. 3 is devoted to the study of star and star cluster distributions. In Sect. 4 we introduce a discussion about the infrared observations of the studied field. Finally, in Sect. 5, we discuss each HII region and in Sect. 6 are presented the conclusions.

2. Observations and results

The Hα observations of the region l = 298°, b = 0° have been made with a 36 cm telescope equipped with a focal reducer and a scanning Fabry-Perot interferometer. This equipment installed at La Silla, of Chile, is devoted to an Hα survey of our Galaxy. A complete description of this equipment and of the reduction techniques can be found in le Coarer et al. (1992). Each observation is a data cube (x, y, λ) covering a 38' x 38' field, with a 9" x 9" spatial resolution. The Fabry-Perot, with interference order 2604, allows a velocity sampling of 5 km s^{-1} and a free spectral range of 115 km s^{-1}.

The wavelength calibration is supplied by an Hα lamp and the shape of the instrumental line profile is given by a neon lamp (since it provides a narrow line at 6598.9 Å compared with Hα lamp). This last profile helps us to map the center to edge widening correction. Some night sky lines (geocoronal Hα and OH 6568.8 Å) are also transmitted through the interference filter used. These lines, which were fitted with an instrumental

Send offprint requests to: D. Russeil

⋆ Based on observations collected at the European Southern Observatory

Table 1. Observations

Obs.	α	δ	date	geo$_{H\alpha}$	OH
	h m s	° '		counts/px/h	
208	12 10 02	-62 32	03/22/92	0.4	0.2
217	12 16 34	-62 39	03/26/92	0.3	0.05
260	12 14 59	-62 08	02/16/93	0.6	0.2
265	12 04 45	-62 52	02/18/93	0.5	0.14
266	12 00 08	-62 59	02/18/93	0.6	0.1
268	11 52 28	-62 51	02/19/93	0.5	0.14
301	12 08 48	-62 57	03/15/93	0.3	0.14
417	12 13 46	-62 44	04/02/94	0.2	0.1
418	12 10 37	-62 10	04/02/94	0.2	0.1
420	12 02 47	-62 25	04/03/94	0.2	0.08
422	11 57 34	-62 54	04/04/94	0.2	0.14
423	11 57 29	-62 19	04/04/94	0.2	0.1
426	11 41 07	-62 10	04/05/94	0.33	0.16
427	11 47 10	-61 56	04/06/94	0.22	0.086
476	12 07 47	-62 27	04/01/95	0.22	0.10
479	12 04 00	-63 24	04/02/95	0.27	0.12
495	11 45 52	-61 52	04/07/95	0.23	0.06

profile, show an intensity varying with time and from one sky region to another. For each observation, an estimation of their intensity is made independently in order to subtract them, from the observed profile.

The data cube reduction method used is described in Georgelin et al. (1994). Table 1 gives the coordinates of the center of each observed field together with the date of observations and mean sky night line intensities. Figure 1 summarizes the results; it shows the map of the ionized gas obtained when adding wavelength channels centered on the Hα emission with positive velocities (V_{LSR} = +25 to + 35 km s^{-1}) for Fig. 1a and negative velocities (V_{LSR} = -25 to -40 km s^{-1}) for Fig. 1b. In addition in Fig. 1c we present the Caswell & Haynes continuum radio map of the same region.

2.1. The HII regions

Most of the HII regions detected in the area studied exhibit a relatively small size. The Hα profile of each HII region is added over its total surface and then fitted with a gaussian profile convolved with the instrumental profile. This Hα profile can then be used to determine the systemic velocity and the doppler width of each discrete HII region.

For each detected HII region we give, in Table 2, the Hα velocity and the FWHM of the deconvolved gaussian together with radial velocities at other wavelength:

- Column 1: Galactic coordinates of the 5GHz continuum radiosources catalogued by Caswell & Haynes (1987).
- Column 2: Equatorial coordinates of the Hα sources.
- Column 3: Estimated Hα diameter.
- Column 4: Hα velocity and width measured in this study.
- Column 5: H109α velocity (Caswell & Haynes 1987).
- Column 6: H_2CO velocity (Whiteoak & Gardner 1974).
- Column 7: CO velocity (Whiteoak et al. 1982; Brand 1986).
- Column 8: OH velocity (Caswell & Robinson 1974).

Two velocity groups are easily identified in this area: the HII region RCW 64 which exhibits a negative velocity and the other ones which exhibit positive velocities placing them beyond the solar circle.

Let us note the case of the Hα emission having apparently no radio nor infrared counterpart. It is well identified on Fig. 1a at coordinates 12^h04^m and -63°24' (l = 297.°93, b = -1.°75). With such a positive velocity this region is far away in spite of its appearance.

2.2. The diffuse emission

A diffuse Hα emission is widely distributed all around the discrete HII regions of the area studied. In order to increase the signal/noise ratio, the profiles were added over extended zones. The obtained profiles were then fitted in the same manner as for discrete HII regions.

The profile decompositions reveal 3 components with negative velocities. The most intense (mean intensity 0.9 counts/px/h) is relatively uniform all over the whole area, its mean velocity is -2.6 km s^{-1}. The mean velocities of the two fainter components are -41 km s^{-1} (varying between -44.3 and -36.8) and -25 km s^{-1} (varying between -21.5 and -29.5). The -25 km s^{-1} component is detected all over the studied area, its mean intensity is 0.4 counts pixel^{-1} hr^{-1} but it can increase twofold inside the same 38' x 38' elementary field; such an increase sometimes significantly changes the profile shape of the observed line. For example we can see from Fig. 1b that the emission is reinforced at 12^h08^m -62°10', 12^h13^m -61°57' and 11^h51^m -62°5'.

The mean intensity of the weakest component is 0.26 counts pixel^{-1} hr^{-1} and in some elementary fields it is not detected at all.

3. Stars and star clusters

In order to obtain information on the distribution of early type stars and on interstellar absorption in this direction, the OB star distances and the visual absorption coefficient have been estimated within an area ranging from l = 296° to 300° and from b = -5.°34 to +5.°86 using data (spectral type and UBV photometry) from the literature (Wramdemark 1980, Deutschman et al. 1976, Savage et al. 1985, Grillo et al. 1992, Garrison et al. 1977, Schild et al. 1983). For young star clusters we choose a slightly wider range of longitude, from l = 294° to 300°; their distances and corresponding A_v were taken directly from the literature (Pandey et al. 1989, Janes & Adler 1982, Hron 1987, Battinelli & Capuzzo-Dolcetta 1991).

For each star, the absolute magnitude has been estimated using the M_v - spectral type relation of Schmidt Kaler (1983) and Humphrey & Mc Elroy (1984). The spectral type found in the literature was preferably used for the M_v deduction. For stars without known spectral type, it has been estimated from UBV photometry and Hβ measurements (Schmidt Kaler 1983). Stars

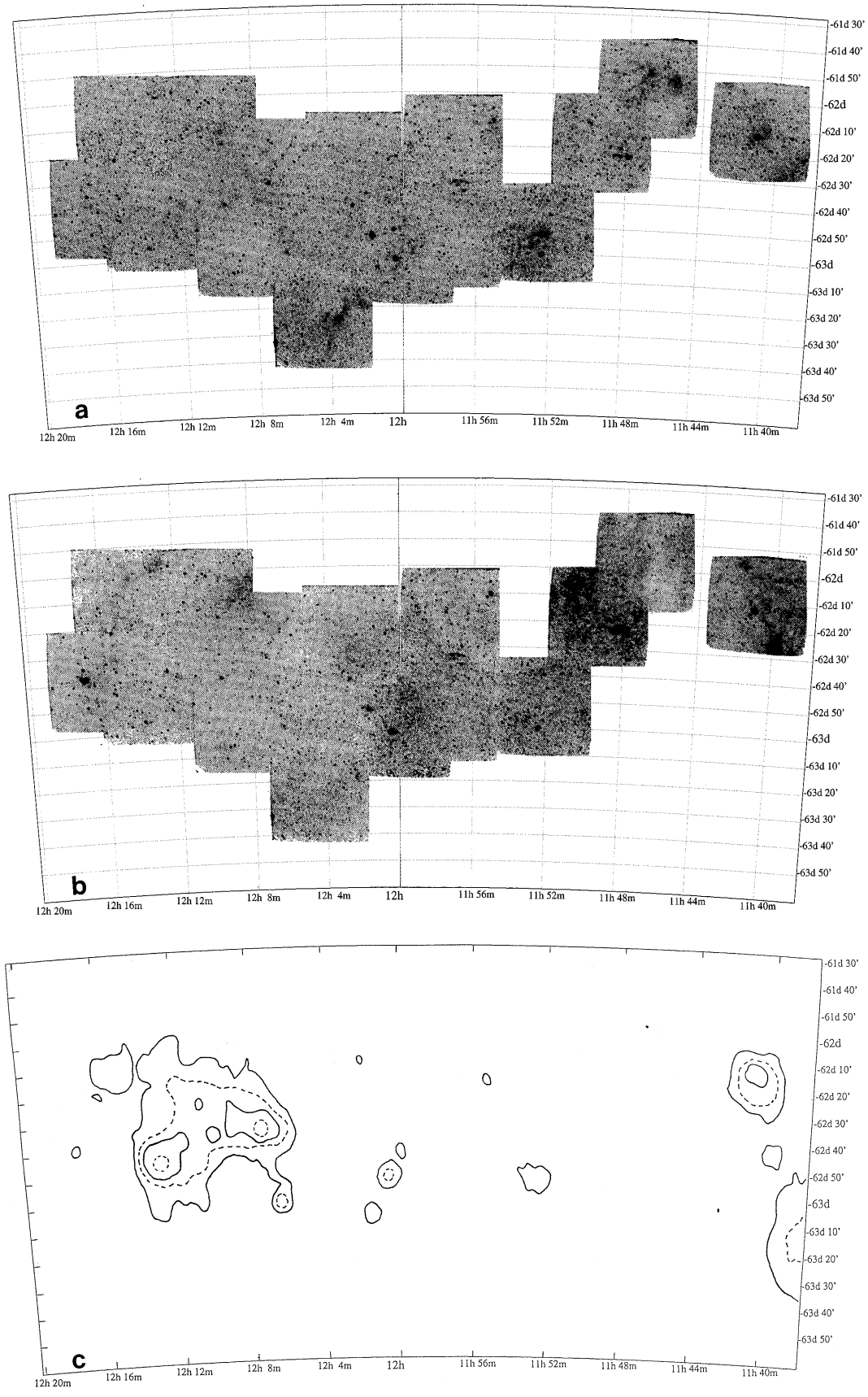

Fig. 1a–c. Monochromatic images (bandwith 0.3 Å) of the Hα emission at positive **a** and negative **b** velocities. In addition the 5GHz radio continuum map of Caswell & Haynes (1987) is presented **c** (contours levels 0.4, 1, 2 and 8 K). Let us note from **b** that the Hα emission around 11^h39^m -62°25' is a part of the large HII region RCW62

Table 2. Integrated Hα velocities and FWHM of discrete HII region. In parallel, H109α, H_2CO and OH velocities are shown

Galactic coordinates of radio sources		Hα (1950)		Hα dim	Hα					
l	b	α	δ		$V_{H\alpha}$	ΔV	$V_{H109\alpha}$	V_{H_2CO}	V_{CO}	V_{OH}
°	°	h m s	° ,	,	km/s	km/s	km/s	km/s	km/s	km/s
295.144	-0.628	11 40 37	-62 11	4.3x2.8	30	25	38			
295.760	-0.200	11 46 45	-61 56	29.3	18	25	17			
296.593	-0.975	11 52 20	-62 52.3	9x9.3	26	25	25			
297.506	-0.765	12 00 31	-62 51.3	2.1x1.6	26	25	23			
297.655	-0.977	12 01 25	-63 5	1.8x2.1	28	29	26	28		
		12 03 31	-63 24	16.1	30	25				
298.187	-0.782	12 06 20	-62 59.3	1.6x1.3	15	30	16			
298.228	-0.331	12 07 14.3	-62 32	1x1	31.6	35	31	-34.9,23.3,30.3	-36.1,34.1	
		12 08 39.5	-62 26	6	31.6	25				
		12 09 09	-62 34	5	23	27				
298.559	-0.114						23			
298.868	-0.432						25	-36.4,19	-37.3,17.4,28.5	26,19
299.016	+0.148						23	23		
299.363 (= RCW 64)	-0.257	12 17 8.6	-62 38.6	3.1x4.3	-40	26	-37		-40.4	

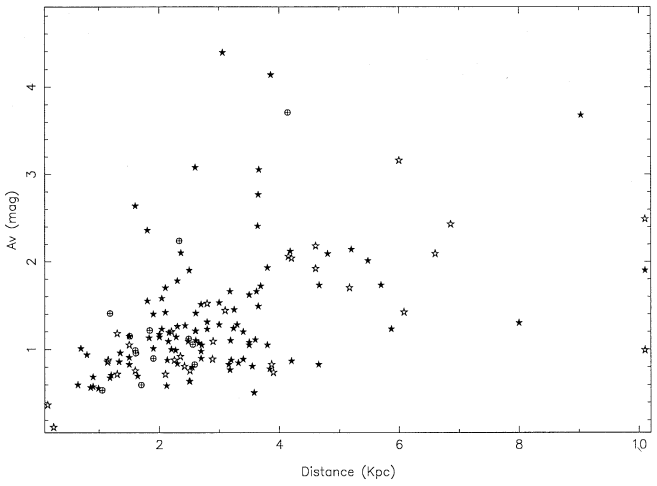

Fig. 2. The visual absorption coefficient of early type stars as a function of the distance. Full star symbols are for stars with UBV photometry alone and open star are for ones with known spectral type, circular symbols corresponds to star clusters

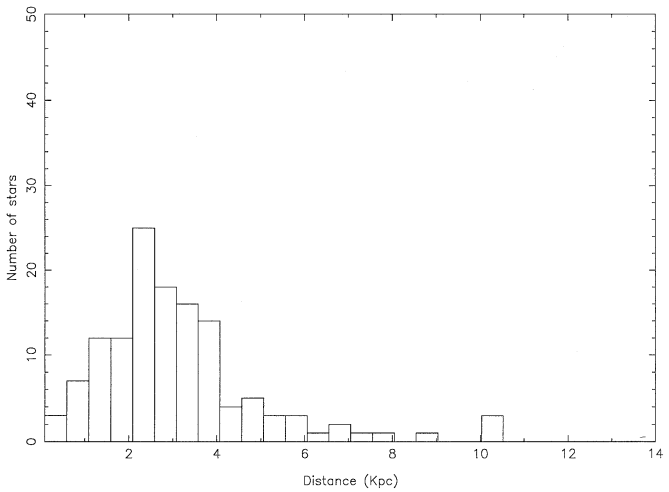

Fig. 3. The frequency distribution of early type stars with distance

with neither spectral type nor Hβ photometry, were arbitrarily supposed to be main sequence stars. Their adopted luminosity thus being a minimum value, the distances of these stars are minimum distances.

The smoothed distribution of A_v (= 3.2 E_{B-V}) as a function of distance displayed on Fig. 2 shows that there is no distinct absorption zone within 4 kpc.

One can see on Fig. 3 that the maximum number of stars lie between 2 and 4 kpc suggesting that the line of sight crosses an arm there. This idea has already been invoked by Mc Cuskey (1983) in order to explain the maximum of the OB star distribution around 2.5 kpc within a 20° side area centered at l = 298° and b = + 1°.

We can note that some stars lie between 4 and 6 kpc. With a wider latitude range, Wramdemark (1980) found some stars with distances greater than 4.5 kpc. One can divide these stars into two groups: the ones with distances between 4.6 and 6.9 kpc and the other ones with distances between 8.6 and 15.9 kpc. This second group can be unambiguously identified with farthest part of the Carina arm. This fact well agrees with the observation of HII regions beyond the solar circle discussed in Sect. 5.4.

As a conclusion, the distribution of early type stars in the l = 298° direction, clearly shows the crossing of the Carina arm at its nearest and farthest parts, but also reveals a bulk of stars at

about 6 kpc. We will see below how this peculiar star distribution can be connected with the ionized emissions detected.

4. The infrared data

Within the studied area, some regions exhibit a high 5 GHz radio emission without any Hα counterpart, meanwhile others with weaker radio emission are detected at Hα wavelength. In order to understand this lack of Hα detection, we compared the infrared data of the different sources in the field. There are two possible cases to explain the absence of Hα emission: either the considered regions are deeply embedded within the molecular cloud where they were born, or some absorbing clouds are distributed along the line of sight.

With regard to the first case, pre main-sequence star(s) create an HII region, the hydrogen being ionized by Lyman continuum photons of massive star(s). The HII region emission lines, and the subionizing stellar flux are then absorbed by dust grains. When the source is deeply embedded in dust, the bolometric luminosity of the star(s) inside the HII region should be roughly equal to the far-infrared luminosity (Codella et al. 1994). No Hα detection should be possible for such embedded sources.

We examine this physical aspect for the radio sources of the studied zone. The far-infrared luminosities are estimated from IRAS calibrated sky flux maps supplied by IPAC. Simulating a circular aperture around each source, we determine the flux in the 12, 25, 60 and 100 μm passbands. The dust color temperature is estimated from the f(60)/f(100) ratio and the total far-infrared luminosity L_{IR} is estimated (Schewring 1989) taking for each region the distance of the associated complex determined in Sect. 5.4. The 5 GHz radio emission (Caswell & Haynes 1987) allows us to estimate the ionizing photon number taking T_e = 10000K (Lequeux 1980). Then the total luminosity L_{tot} of a single star that would be required to ionize the HII region is inferred from Thompson's (1984) conversion table. The infrared measurements, total luminosity and color temperature for each source are given in Table 3.

First we can compare the far-infrared color indexes, estimated from the IRAS fluxes, with the existing criteria used for classifying HII regions as normal (Hughes & Mac Leod 1989) or ultra compact (Wood & Churchwell 1989) (respectively labeled HII and UC in Table 1).

Most of the region studied fulfil both the ultra compact and the classical HII regions criteria. It has been shown that more diffuse HII regions also satisfy the Wood & Churchwell criteria (Codella et al. 1994).

Surprisingly RCW 64 (= G 299.363 - 0.257) does not satisfy any of these criteria. Let us note that the infrared emission of RCW 64 seen on IRAS maps is probably contaminated by a nearby infrared emitting object.

Amid far HII regions detected in Hα the more extended Hα emissions (295.76, 296.593) have a high luminosity ratio L_{tot}/L_{IR}. This fact can be linked to the HII region evolution. When an HII region ages, the dust is progressively destroyed and the region spreads. For young embedded objects, a luminosity ratio of 1 is expected. Amongst the 3 regions of the distant complex which have a luminosity ratio below one, two exhibit an Hα counterpart. It is hard to know whether these values are significant or due to uncertainties in the infrared measurements or to IRAS map calibration effects. The luminosity ratio of the regions not detected at Hα wavelength is not significantly different from the other ones. Since they are found in the same part of the field, this suggests that the lack of Hα detection is due to absorbing interstellar cloud rather than to circumstellar matter.

The IRAS map investigation, has exhibited four extended infrared sources without radio nor Hα counterpart. The coordinates of the center of these sources, measured from IRAS maps, are 12^h08^m -62°11', 11^h56^m -63°21', 12^h01^m -62°21' and 11^h57^m -62°47'. IRAS sources which are not seen in radio continuum may be BN type objects, molecular cores or dark clouds. We compared far-infrared colors of the 4 IRAS sources to the color criteria determined by Henning et al. (1990), Emerson (1987) and Chini et al. (1986) and found 2 sources fullfilling no criteria and 2 others fullfilling both BN-type object and molecular core criteria. In addition their color temperature (above 20K) and their 100 μm flux (above 500 Jy) suggest that these sources are not associated with dark clouds (Chini et al. 1986). Then their real nature remains to be determined.

5. Discussion

5.1. The -2.6 km s^{-1} *diffuse component*

Detected all over the area studied, the -2.6 km s^{-1} component is the main diffuse Hα emission. Its intensity is, respectively, 3 and 8 times that of the Hα and OH night sky lines, and its velocity (V_{LSR}) ranges from -0.6 to -5 km s^{-1}. A diffuse component with a V_{LSR} of - 4 km s^{-1} has already been detected at l = 303° (le Coarer et al. 1992). Such a diffuse component may be the ionized counterpart of the nearby interstellar medium. An expansion motion of this interstellar medium has been shown (Crawford 1991) from the NaI and CaII absorption lines observed in the direction of 28 stars of the OB Sco-Cen association. Most of the components detected by Crawford exhibit negative velocities which are interpreted as matter out-flows due to the mass loss of the most massive stars of the association. Particularly, within the longitude range 295°- 325°, he shows several components with V_{LSR} between -4 and 0 km s^{-1} which can be associated with an envelope related to the Lower Centaurus Crux subgroup (LCC) (Blaauw 1964).

The -2.6 km s^{-1} diffuse Hα component is probably associated with this LCC subgroup at 130 pc (Degeus et al. 1989) and we can place it at the inner part of the local spiral arm.

5.2. The -25 km s^{-1} *diffuse component*

This emission is found all over the field with a -25 km s^{-1} mean velocity (velocity range: -21.5 to -29.5). The rotation model used (Brand & Blitz 1993), gives two likely kinematical distances for this emission: 5.2 kpc or 2.8 kpc.

We detected no discrete HII region with this velocity. However, some small regions, itemized by Brand (1986) exhibit CO velocity of the same nature: BBW 374 (V_{CO} = -26.3 km s^{-1},

Table 3. Infrared observations

Name	$f_{12\mu m}$ Jy	$f_{25\mu m}$ Jy	$f_{60\mu m}$ Jy	$f_{100\mu m}$ Jy	T_D K	Log $L_{tot}/L_\odot$	Log $L_{IR}/L_\odot$	L_{tot}/L_{IR}	Remarks
295.144	356.67	1591.21	10405.2	14870.0	36.4	6.42	6.33	1.23	UC - HII
295.760	4.63	30.6	255.7	322.4	38.23	5.88	4.70	15.1	UC - HII
296.593	25.24	68.22	647.7	999	35.3	5.84	5.10	5.49	HII
297.506	90.7	317.9	2271.5	3408.5	35.7	5.71	5.68	1.07	$\sim$ UC - HII
297.655	36.35	126.74	1097.056	1628.00	35.86	5.44	5.36	1.20	$\sim$ UC - HII
298.187	79.12	465.04	2029.73	2193.19	40.86	5.57	5.58	0.97	UC - HII
298.228	1237.41	6851.9	21965.4	21754.4	42.5	6.55	6.61	0.87	$\sim$ UC - HII
298.868*	1096.76	6042.64	31910.26	37905.0	39.2	6.63	6.79	0.77	UC - HII
298.559*	30.68	122.41	1087.8	1617.0	35.8	5.63	5.36	1.86	UC - HII
299.016*	51.76	132.45	1228.3	2160.5	33.7	5.60	5.45	1.41	HII
RCW64	83.74	102.72	1091.91	2157.5	32.33	4.81	4.89	0.83	

Notes:
Column 2 to 5: the fluxes are color corrected (IRAS Explanatory Supplement, 1985)
*: sources not detected in Hα
$\sim$ UC: sources with infrared color indexes near the UC criteria

$d_\star$ = 3.28 kpc), BBW 377 (V_{CO} = -29.8 km s^{-1}, $d_\star$ = 2.9 kpc) and BBW 384 (V_{CO} = -25.7 km s^{-1}, $d_\star$ =1.86 kpc). The two first regions are outside the area studied; the third one exhibits no Hα counterpart, suggesting that it is a reflection nebula.

In addition, a molecular cloud at l = 294°, b = -1.5° exhibiting a -25 km s^{-1} velocity (Cohen et al. 1985) and the large complex RCW 60-61-62 associated with the star group IC 2944 (Ardeberg & Maurice 1981) are at a distance of 2.5 kpc.

From the stellar distribution study (Sect. 3) we have found a maximum of early type stars at 2.5 kpc. We adopt this distance for the Hα diffuse component at -25 km s^{-1}. This diffuse emission allows us to link the Carina and Sagittarius spiral features. Humphreys (1972) already suggested that the presence of many supergiants between 2 and 4 kpc from the Sun might be an optical link between these spiral features.

Let us note that in this direction the diffuse component we detected is the unique velocity tracer of the nearest part of the Sagittarius-Carina arm.

5.3. RCW 64 (= G 299.363 - 0.257) and the -40 km s^{-1} diffuse component

This HII region, although rather bright at Hα wavelength, is barely detectable in radiocontinuum and on IRAS images. Its measured Hα velocity (V_{LSR} = -40 km s^{-1}) is close to the H 109α (Caswell & Haynes 1987) and CO (Brand 1986) velocities (respectively -37 km s^{-1} and -40.4 km s^{-1}). CO studies of Grabelsky (1988) show a maximum emission at l = 299.375° and b = -0.25°, with a -40 km s^{-1} velocity. This CO molecular cloud is probably associated with RCW 64. Besides, from Table 2, one can see that H_2CO and CO velocity components measured in the direction of some other HII regions are in good agreement with this molecular cloud presence. Let us note, also, that a diffuse emission is detected at -41 km s^{-1} at many places of the studied area.

Taking the Brand & Blitz (1993) Galactic rotation curve, with an orbital velocity of 220 km s^{-1} at the Sun radius (8.5 kpc), the RCW 64 velocity, exhibits a strong departure from the circular rotation, whatever the tracer used, which stops one from making any kinematical distance determination. Let us recall that the tangential point distance is 4.2 kpc in this direction, implying a minimum theoretical radial velocity of -30.3 km s^{-1}, which is already 10 km s^{-1} higher than the observed velocity. Such departure to pure circular rotation is found whatever the model of Galactic rotation used. It has been already mentioned by several authors (Humphreys 1971, Humphreys 1972, Alvarez et al. 1990, Brand & Blitz 1993). For example, Alvarez et al. (1990) exhibit, from CO terminal velocity measurements between l = 280° and 312°, velocities more negative by about 12 km s^{-1} than within the longitude domain 312° - 346°, a similar departure was also found by Brand & Blitz (1993) between l $\sim$ 275° and 305° (limit of their sample).

Fortunately, Brand (1986) identified some exciting stars of RCW 64 and derived a stellar distance of 5.37 kpc.

The galactic coordinates and distance of RCW 64 and its associated molecular cloud and stars place it between Carina and Centaurus arm. Then we cannot deduce to which arm it actually belongs. It may well be a spur between two arms (as one can observe in many other spiral galaxies). In order to confirm and delineate this possible spur, other Hα observations between galactic longitude 300° and 310° are needed.

5.4. The distant sources

Most of the sources detected at Hα wavelength have positive velocities, which in this direction place them outside the solar circle. It is the first time that so many distant HII regions are detected. For all of these sources $V_{H\alpha}$ and $V_{H109\alpha}$ are in good agreement, and the Hα emission coincides fairly well with the radio continuum map. We discuss here some HII regions of spe-

cial interest :

G 295.144 - 0.628

This region exhibits intense and extended radio and infrared emission. Its color indexes are those of a classical HII region despite its relatively low luminosity ratio (Table 3). We find an Hα velocity of 30 km s^{-1}, quite different from the H109α velocity (38 km s^{-1}). The velocity measured at Hα wavelength shows that this region is possibly associated with the complex at 10 kpc.

G 295.760 - 0.200

This small Hα emission is easily detected and coincides with very weak IRAS and radio emissions (it is the weakest radio source investigated by Caswell & Haynes 1987) and exhibits the highest L_{tot}/L_{ir} ratio (see Table 3). This source is surrounded by an extended Hα emission at the same velocity, without any radio continuum counterpart. It is impossible to know whether this emission is more extended, and forms for instance a shell around the source, because the line of sight almost crosses the dark cloud DC 295.8 - 0.3 seen to the Southwest of the region.

G 297.506 - 0.765 and 297.655 - 0.977

Both sources exhibit compact Hα emission. A nebula of 43' x 17' size (BBW 379), situated between these sources, has been itemized by Brand (1986), who linked it with the 3° x 3° Hα region centered around 297.7 - 0.4 (Georgelin & Georgelin 1970). He made a CO velocity measurement of 30.8 km s^{-1} between these two radio sources (l = 297.58°, b = -0.87°) however we detect no Hα emission with positive velocity there. This CO emission is probably associated with the distant sources but not with the HII region detected by Brand which is certainly a local maximum of the Hα diffuse emission with V_{LSR} = -2.6 km s^{-1}.

[297.93 - 1.75] (12^h3^m5 -63°24')

Extended Hα emission, not mentioned in the literature, can be seen at $12^h03^m31^s$ -63°24' on Fig. 1a without any known counterpart in the radio continuum or infrared counterparts. It has a positive velocity and exhibits a small gradient: the brighest part being found at 30 km s^{-1} and the faintest one at 23 km s^{-1} .

G 298.187 - 0.782

This small, very bright, Hα source exhibits the smallest velocity and a slightly larger than average Doppler broadening. It also appears as a strong source on radio surveys (Caswell & Haynes 1987). Its true nature still remains unclear: planetary nebula (it is known as He 2 - 77 or PK 298 - 0.1) or normal HII region? In early observational studies it has been classified as a suspected planetary nebula (Sanduleak 1976). De Muizon (1988) finds the presence of far-infrared emission lines of ionisation stages commonly observed in planetary nebulae but not seen in HII regions, a total infrared luminosity between 1250 and 1800 $L_\odot$ and a mass of gas estimated to 6 10^{-2} $M_\odot$ assuming a distance of 0.5 kpc. Then she suggests that this source is a planetary nebula rather than a compact HII region. However, the fact that it follows the infrared color criteria of Wood & Churchwell (1989) and Hughes & Mac Leod (1980) (see Sect. 4) and not those of Planetary nebulae (Emerson 1987) suggests it is an HII region. Moreover the kinematic studies leading to a 9.5 kpc distance, significantly modify the physical values. Adopting this last value of distance, the total infrared luminosity and the mass of gas values become respectively 5 10^5 $L_\odot$ and 22 $M_\odot$ which are typical of normal HII regions. Caswell & Haynes (1987) from electron temperature and observed flux density at 5 GHz already argued that it is a normal HII region.

G 298.228 - 0.331

This region has strong infrared and continuum radio emission, but is barely visible in our Hα survey field. Its very small angular dimension, and the bright star found almost in the same line-of-sight, render the Hα profile extraction tricky. Nevertheless, it is the first HII region of this distant complex detected at Hα wavelength using a higher spatial resolving instrument (Georgelin et al. 1979). Two extended Hα emission regions are detected in the same field: around 298.43° - 0.35° ($12^h09^m9^s$, -62°34') and 298.36° - 0.22° ($12^h08^m39.5^s$, -62°26') which are almost certainly connected with the 298.228° -0.331 radio continuum extension. These two Hα emissions exhibit respective velocities of 23 km s^{-1} and 31.6 km s^{-1}, comparable with the velocities of the other emissions.

Except G 295.760 and G 298.187 all of the distant HII regions have velocities between +23 and + 31 km s^{-1}, suggesting that they belong to the same large complex. This complex may be related to the two molecular complexes presented by Grabelsky (1988) number 26 (l = 298.8° b = 0.2°) and 24 (l = 297.4° b = -0.5°) with respective velocities 25 km s^{-1} and 21.5 km s^{-1}. From the point of view of the galactic structure, these HII regions and molecular clouds can be grouped into a single complex, at a distance of 10 kpc using a flat rotation curve, $R_\odot$ = 8.5 kpc and $\theta_\odot$ = 220 km s^{-1}. This complex is fairly well located on a logarithmic spiral of 12° pitch angle, tracing the Carina arm.

G 295.76 and G 298.187 exhibit significantly different velocities (see Table 2). Their belonging to the same complex is far from proved. Moreover, H_2CO, OH and CO measurements given in Table 2, show some velocities with values significantly lower than 24 km s^{-1}, suggesting that there is another complex in the line of sight which may includes G 295.76 and G 298.187. However their individual kinematical distances lead to the values of distances 9.2 and 9.5 kpc, allowing them to still belong to the Carina arm. We conclude that all the HII regions of this study with positive velocities most probably belong to the farthest part of Carina arm.

6. Conclusion

The various spiral structure tracers studied, at galactic longitude l = 298°, permitted us to investigate both near and far Carina arm parts. The near part of this arm is only detected from diffuse ionized gas, largely observed all over the studied area at -25 km s^{-1}. No discrete HII regions being found at this velocity, it is the first time that an interstellar tracer of the spiral structure allows us to link the Carina arm to the Sagittarius arm in this direction.

The far part of the Carina arm is detected thanks to distant HII regions with positive velocities. The optical detection of such far regions confirms that the line of sight mostly remains

between two spiral arms. Both distance crossing of this spiral arm well agree with a logarithmic spiral of 12° pitch angle.

In the zone studied, the RCW 64 region exhibits a clear departure from circular rotation ; its stellar distance places it between the Carina and Scutum-Crux arms. Furthermore the detection of associated diffuse Hα emission and the bulk of young stars encountered between 4.6 and 6.9 kpc suggest that there is a spur between the Carina and Scutum-Crux arm in this direction. Observations at higher longitude should enable us to find which arm it belongs to.

Because of absorption we do not detect Hα counterparts of 4 radio sources of this far complex. Since the main absorption cause is dust we have used IRAS data in order to compare the absorption conditions for the different sources. No obvious difference has been found, but our sample is too small to draw clear conclusions about the absorption effects.

Besides some IRAS sources have no radio nor Hα counterpart. A systematic study of such objects will be made in order to determine their nature and their possible link with HII regions and molecular clouds.

Acknowledgements. The author wishes to thank the following persons involved in the observations: P. Amram, Y.M. and Y.P. Georgelin, G. Goldes, E. Le Coarer and M. Marcelin.

References

Alvarez H., May J., Bronfman L., 1990, ApJ 348, 495
Ardeberg A., Maurice E., 1981, A&A 98, 9
Battinelli P., Capuzzo-Dolcetta R., 1991, MNRAS 249, 76
Blaauw A., 1964, ARA&A 2, 213
Brand J., 1986, Ph. D. Thesis, University of Leiden
Brand J., Blitz L., 1993, A&A 275, 67
Cameron B., Thomas C., 1991, PASP 103, 1094
Caswell J.L., Robinson B.J., 1974, Aust. J. Phys. 27, 597
Caswell J.L., Haynes R.F., 1987, A&A 171, 261
Chini R., Kreysa E., Krügel E.G., Mezger P.G.,Gemünd H.P., 1986, Light on Dark matter, Ed. F.P. Israël, Ap&SS Library p. 29
le Coarer E., Amram P., Boulesteix J. et al.,1992, A&A 257, 389
Codella C., Felli M., Natale, V., 1994, A&A 284, 233
Cohen R.S., Grabelsky D.A., Alvarez H. et al.,1985, ApJ 290, L15
Crawford I.A., 1991, A&A 247, 183
Degeus E.J., de Zeeuw P.T., Lub J.,1989, A&A 216, 44
Degeus E.J., Vogel S.N., Digel S.W., Gruendl R.A., 1993, ApJ 413, L97
De Muizon M.J., 1988, Thesis
Deutschman W.A., 1976, ApJ 30, 97
Emerson J.P., 1987, IAU Symp. 115, 19
Fernie J.D., 1983, ApJS 52, 7
Garrison R.F., Hiltner W.A., Schild R.E., 1977, ApJS 35, 111
Georgelin Y.P., Georgelin Y.M., 1970, A&A 6, 349
Georgelin Y.M., Georgelin Y.P., Sivan J.P., 1979, IAU Symp. 84, 65
Georgelin Y.M., Boulesteix J., Georgelin Y.P., le Coarer E., Marcelin M., Monnet G., 1988, A&A 190, 61
Georgelin Y.M., Amram, P., Georgelin Y.P., le Coarer E., Marcelin M.,1994, A&AS 108, 513
Grabelsky et al., 1988, ApJ 331, 181
Grillo F., Sciortino S., Micela G., Vaiana G.S., 1992, ApJS 81, 795
Haynes R.F., Caswell J.L., Simons L.W., 1978, Aust. J. Phys. Suppl. 45, 1
Henize K.G., 1967, ApJS 14, 125
Henning Th., Pfau W., Altenhoff W.J., 1990, A&A 227, 542
Hron J., 1987, A&A 176, 34
Hughes W.A., Mac Leod G.C., 1989, AJ 97, 786
Humphreys R.M., 1971, ApJ 163, L111
Humphreys R.M., 1972, A&A 20, 29
Humphreys R.M., McElroy D.B., 1984, ApJ 284, 565
IRAS Explanatory Supplements, 1985, Joint IRAS Science Working Group, ed. Beichmann C.A et al., US Govt Printing Office
Janes R, Adler D., 1982, ApJS 49, 425
Lequeux J., 1980, in Star formation, edited by A. Maeder & L. Marnet (Geneva Observatory, Sauverny) 77
McCuskey S.W., 1983, AJ 88, 1175
Meynet G., Mermilliod J.C., Maeder A., 1983, A&AS 98, 477
Pandey A.K., Bhatt B.C., Mahra H.S., Sagar R., 1989, MNRAS 236, 263
Sanduleak N., 1976, Publ. Warner & Swasey Obs. 2, 56
Savage B.D., Massa D., Meade M., 1985, ApJS 59, 397
Schewring P.B.W., 1988, Thesis, Sterrewacht
Schild R.E., Garrison R.F., Hiltner W.A., 1983, ApJS 51, 321
Schmidt Kaler Th., 1983, Landolt-Bornstein, New Series, Group VI, Vol. 23 (Springer) 14
Thompson R.I., 1984, ApJ 283, 165
Whiteoak J.B., Gardner F.F., 1974, A&A 37, 389
Whiteoak J.B., Otrupcek R.E., Rennie C.J., 1982, Proc. Astron. Soc. Aust. 4, 434
Wood D.O.S., Churchwell E., 1989, ApJ 340, 265
Wramdemark S., 1980, A&AS 41, 33

This article was processed by the author using Springer-Verlag LaTeX A&A style file *L-AA* version 3.